Scientific Papers of
the Department of Electrical Power Engineering of
the Wrocław University of Science and Technology

PRESENT PROBLEMS OF POWER SYSTEM CONTROL

8

Wrocław 2017

Cover design
Piotr PIERZ

Printed in the camera ready form

Department of Electrical Power Engineering
Wrocław University of Science and Technology
Wybrzeże Wyspiańskiego 27, 50-370 Wrocław, Poland
phone: +48 71 320 35 41
www: http://www.weny.pwr.edu.pl/instytuty,52.dhtml; http://www.psc.pwr.edu.pl
e-mail: wydz.elektryczny@pwr.edu.pl

OFICYNA WYDAWNICZA POLITECHNIKI WROCŁAWSKIEJ
Wybrzeże Wyspiańskiego 27, 50-370 Wrocław
http://www.oficyna.pwr.edu.pl
e-mail: oficwyd@pwr.edu.pl
zamawianie.ksiazek@pwr.edu.pl

ISSN 2084-2201

Print and binding: beta-druk, www.betadruk.pl

CONTENTS

synchrophasor estimation, dynamic phasor,
Fourier transform, Taylor–Fourier series,
phase-locked-loop, dynamic filter,

Mirosław ŁUKOWICZ*
Szymon CYGAN*

ANALYSIS OF SYNCHROPHASOR ESTIMATION ERRORS

This papers discusses the analytical analysis of the synchrophasor estimation employed in electrical systems. Short time Fourier transform with the phase locked loop and Taylor Fourier series are analyzed for signals relating to different states which may occur in real power systems. The object is the accurate phasor estimation regardless of the shape of input signal, what for some signal types is cumbersome.

As a result of active and reactive power disturbance in a power system, the frequency deviation and amplitude fluctuations may appear in power system signals. As a consequences of short circuits or overvoltages signal changes occur. This leads to unacceptable errors in short time Fourier transform resulting from Fourier transform properties. This paper presents character of occurring errors and their consequences individually for any signal deviation.

1. INTRODUCTION

An accurate estimation of electrical signal parameters is a vital issue in power system control and protection. Unbalance between the power supply and the load can lead to dynamic changes of the system state, thus voltage and current magnitudes, wave shapes as well as the actual system frequency can vary from nominal values. The efficient control of an electrical network requires more and more accurate information about signal parameters. This include the accurate measure of the phase, the magnitude, the frequency, higher harmonics, Rate of Change of Frequency (ROCOF) and the magnitude change rate. These parameters can be represented in the concise form as a complex valued function referred to as a phasor.

* Wrocław University of Science and Technology, Department of Electrical Power Engineering, Wybrzeże Wyspiańskiego 27, 50-370 Wrocław, Poland, e-mail: miroslaw.lukowicz@pwr.edu.pl, szymon.cygan@pwr.edu.pl

According to synchrophasor standard C37.118.2011 [1], two base classes of estimating algorithms have been defined: P (protection) and M (measurement) class. Both classes are diversified by purpose of application, i.e. P class is designed for cooperation with power system relays. These algorithms are designed to give quick responds to changes in the input signal and to damp response overshoots. M class algorithms are designed for accurate phasor estimation for all signals mentioned in the synhrophasor standard. Requirements for the response time and the acceptable overshoot are milder.

Phasor estimation problem is a well studied issue. The fundamental technique of phasor estimation is based on Short Time Fourier Transform (STFT) of an input signal. STFT is an efficient and a potent way for phasor estimation as long as the frequency of a measured signal does not differ from nominal 50 Hz and a signal amplitude is constant. Occurrence of minor frequency changes yields to disturbance of the algorithm response with the second harmonic and unacceptable estimation errors. The amplitude of the second harmonic is proportional to the difference Δf between the nominal frequency 50 Hz and the actual frequency of the processed signal. The influence of second harmonic distortion can be damped by using a well designed filter or extending integration time in STFT. However, extension of the integration time leads to delay of reporting, and the use of additional filters makes the dynamic more complex. Many different techniques have been used for the proper design of STFT dedicated filters. One approach is based on the expected filter characteristic [2], [3]. This technique allows for adjusting filter properties according to requirements yet does not allow reduction of errors for all expected conditions. The main advantage of windowed STFT algorithms is a low computation cost and an easy implementation.

The vulnerability to frequency variations can be reduced by applying multilevel STFT algorithms [4], as well as algorithms with adaptive filters [5]. In this method the frequency estimate from the previous step is used for the following phasor estimation using the new basis function. This approach increases the algorithm complexity and the numerical burden, but allows obtaining similar estimation errors for full frequency spectrum as for 50 Hz.

The approach based on Taylor phasor approximation has been studied in [6]–[8]. Evaluating of phasor using Least Squares Method (LSM) and approximating of phasor with a polynomial reduce errors caused by the frequency distortion and the amplitude fluctuation, however estimation errors still increase when the frequency distortion rises. This problem can be damped by using the dynamically changing base function in Taylor series based on the previous phasor analysis [9] or the initial STFT evaluation [10]. However, this solution radically increases computational complexity. The crucial issue for Taylor method is the proper adjustment of the polynomial approximation order of Taylor series. The increase of the polynomial order improves the approximation precision and thereby the algorithm accuracy. However, it greatly increases computational burden, requires special approaches to ensure numerical calculation, and leads to the vulnerability to the signal noises. The vulnerability to noises is caused by improved capability to approximate noised function with polynomials of higher orders.

2. PHASOR ANALYSIS

The dynamic phasor has been introduced in [1] as a concept for representation of a complex input signal. Expressing a fast varying real signal as a slow varying complex signal facilitates an analysis. The dynamic phasor is defined for special set of functions such as

$$x(t) = X_m(t)\cos\left(2\pi\int f(t)\mathrm{d}t + \varphi\right) \tag{1}$$

where X_m denotes a varying amplitude of the input signal, φ stands for a constant phase shift, $f(t)$ designates a real time varying frequency of the signal, f_0 is equal to fundamental frequency $\omega = 2\pi f_0$. For each function (1) the dynamic phasor is formulated as

$$X(t) = X_m(t)e^{2\pi i\int (f(t)-f_0)\mathrm{d}t + i\varphi} \tag{2}$$

It can be easily seen that for each real valued signal, the corresponding phasor fulfills following condition. The fundamental component of the input signal is the real part of the rotating phasor

$$x(t) = \mathrm{Re}(X(t)e^{i\omega t}) \tag{3}$$

therefore the phasor is formulated as

$$X(t) = X_m(t)e^{i\psi(t)}) \tag{4}$$

where $\psi(t)$ is a real valued function which denotes the total instantaneous phase shift.

The definition of the dynamic phasor is correct yet incomplete. Therefore, the extra assumption regarding the frequency has to be made to provide the more precise definition. The notation of function in (2) is not unique. Using trigonometric identities the base sinusoidal signal can be expressed with many significantly different forms. Let us consider the sample sinusoidal signal with the nominal frequency 50 Hz, and constant both the amplitude and the phase shift as follows:

$$x(t) = \sin(\omega t) \tag{5}$$

Corresponding to [1] model phasor defined for model signal is of the form (6). Using sample mathematical operations forms (7) and (8) can also be obtained as phasors fulfilling required criteria.

$$x(t)=\cos\left(\omega t-\frac{\pi}{2}\right) \qquad \begin{gathered} X_m(t)=1 \\ e^{i\psi(t)}=e^{-i\frac{\pi}{2}}=-i \end{gathered} \tag{6}$$

$$x(t)=2\sin\left(-\frac{\omega t}{2}\right)\cos\left(\frac{\omega t}{2}\right) \qquad \begin{gathered} X_m(t)=2\sin\left(\frac{\omega t}{2}\right) \\ e^{i\psi(t)}=e^{-i\frac{\omega t}{2}} \end{gathered} \tag{7}$$

$$x(t)=2\sin\left(\frac{\pi}{2}-\frac{\omega t}{2}\right)\cos\left(\frac{\omega t}{2}-\frac{\pi}{2}\right) \qquad \begin{gathered} X_m(t)=2\sin\left(\frac{\pi}{2}-\frac{\omega t}{2}\right) \\ e^{i\psi(t)}=e^{-\left(\frac{\omega t}{2}+\frac{\pi}{2}\right)} \end{gathered} \tag{8}$$

In fact, infinitely many different forms can express the sinusoidal signal just by using trigonometric formulas. This inaccuracy is crucial problem for complete and accurate phasor estimation as far as any input signal is concerned. The most important issue in the phasor estimation is to define the phasor in such a way to get the unique formula for any real valued function.

In C37.118.2011 the phasor uniqueness has been guaranteed by restricting possible forms of the amplitude and the phase shift concerned as time functions, and dividing model functions into the steady state and dynamic functions. The model of the phasor for a steady state is defined as follows

$$\begin{gathered} x(t)=X_m\cos(\omega_0 t+\varphi)+X_m^k\cos(k\omega_0 t+\varphi_k) \\ X(t)=X_m e^{i\omega_0 t+\varphi} \end{gathered} \tag{9}$$

The phasor amplitude X_m is any positive constant whereas the phasor phase shift φ is a constant from the range $[0, 2\pi)$. The phasor angular speed ω_0 is constant and it does not differ from nominal frequency more than fixed value that depends on the algorithm type. The harmonic distortion is described by harmonic amplitude X_m^k, which also depends on the algorithm employed. The phasor models for the dynamic states have been defined as follows

$$\begin{gathered} X_m(t)=X_m(1+at) \\ X_m(t)=X_m(1+a\chi_{(0,\infty]}(t)) \\ X_m(t)=X_m(1+a\times\cos(\omega_1 t)) \end{gathered} \tag{10}$$

where $X_m(t)$ is a polynomial of order 1, or the step function, or the cosine wave. The phase shift variability can be characterized with the polynomial of order 2, the step function, or cosine function as follows

$$\psi(t) = \psi_0(1 + a_1 t + a_2 t^2)$$
$$\psi(t) = \psi_0(1 + a\chi_{(0,\infty]}(t)) \tag{11}$$
$$\psi(t) = \psi_0(1 + a \times \cos(\omega_1 t))$$

The aforementioned definition under appropriate assumptions for a and ω_1 coefficients provides unique representation for each function from standard test class, but does not cover all periodic functions. There exist reasonable periodic functions which phasors do not belong to the standard class.

Another problem coming with the phasor definition is a constricted reversibility. Let us assume that there are two periodic real valued signals formulated as follows

$$x_1(t) = X_{m_1}(t)\,\mathrm{Re}(e^{i\omega t} e^{i\varphi_1(t)})$$
$$x_2(t) = X_{m_2}(t)\,\mathrm{Re}(e^{i\omega t} e^{i\varphi_2(t)}) \tag{12}$$

which are close to each other in L^2 norm and RMS of their difference is close to zero. The small RMS of the function difference does not imply small amplitude and phase differences. Though functions $x_1(t)$ and $x_2(t)$ are almost equal, their phasors can be significantly different. Therefore, restricted function values lead to the numerically ineffective reversibility.

3. PHASOR ESTIMATION

3.1. PROBLEM DEFINITION

The phasor estimation is a process of finding the corresponding phasor for input signal, based on finite number of probes. For any input signal $x(t)$ it is necessary to find the amplitude $X_m(t)$ and the phase shift $\varphi(t)$ which are close to values of the model. Every phasor estimation algorithm has three main parameters, which describe algorithm efficiency, namely: the Total Vector Error (*TVE*), the Frequency Error (*FE*) and the Rate of Change of Frequency Error (*RFE*). *TVE* is defined as the relative difference between estimated phasor $\hat{X}(t)$ and model phasor $X(t)$. *TVE* is an indicator characterizing absolute difference between estimated and real phase shift as well as between estimated and real amplitude.

$$TVE = \frac{\left|\hat{X}(t) - X(t)\right|}{\left|X(t)\right|} \tag{13}$$

FE is defined as a relative difference between the model frequency and its estimated value.

$$FE = \frac{\left|\hat{f} - f_{\mathrm{real}}\right|}{\left|f_{\mathrm{real}}\right|} \tag{14}$$

RFE is defined in the analogous way as

$$RFE = \frac{\left|d\hat{f} - \dfrac{df_{\mathrm{real}}}{dt}\right|}{\left|\dfrac{df_{\mathrm{real}}}{dt}\right|} \tag{15}$$

Indices *TVE*, *FE*, *RFE* can be roughly interpreted as relative differences between zero, first and second derivative of the complex valued function. The main goal for each estimation algorithm is to keep *TVE*, *FE* and *RFE* as small as possible for all functions in the model function set.

3.2. TEST SIGNAL

Algorithms presented in this paper have been analyzed for signals presented in the model class set. All tests have been performed for boundary signals in the model set class to exhibit estimation problems occurring for these signals. The test signal is presented in Fig. 1, in the form of the model phasor. The signal is composed of 34 different model signals of the critical behavior. Model signals are numbered on *x* axis. The first diagram shows input signal frequency, the second and third ones show the real and imaginary parts of the model phasor. The model signal has been arranged as follows:

- 1 sinusoidal 50 Hz wave with amplitude of 1,
- 2, 3 sinusoidal 48 Hz and 52 Hz waves with amplitude of 1,
- 4–9 sinusoidal 50 Hz waves with ramp of amplitude,
- 10–15 sinusoidal waves with ramp of frequency,
- 16–20 sinusoidal waves distorted with higher harmonics
- 21–24 sinusoidal waves with step changes of amplitude
- 25–28 phase step changes,
- 29 phase oscillation,
- 30 amplitude oscillation,
- 31–34 sinusoidal waves of frequency 45, 50, 55 Hz and amplitude 1.

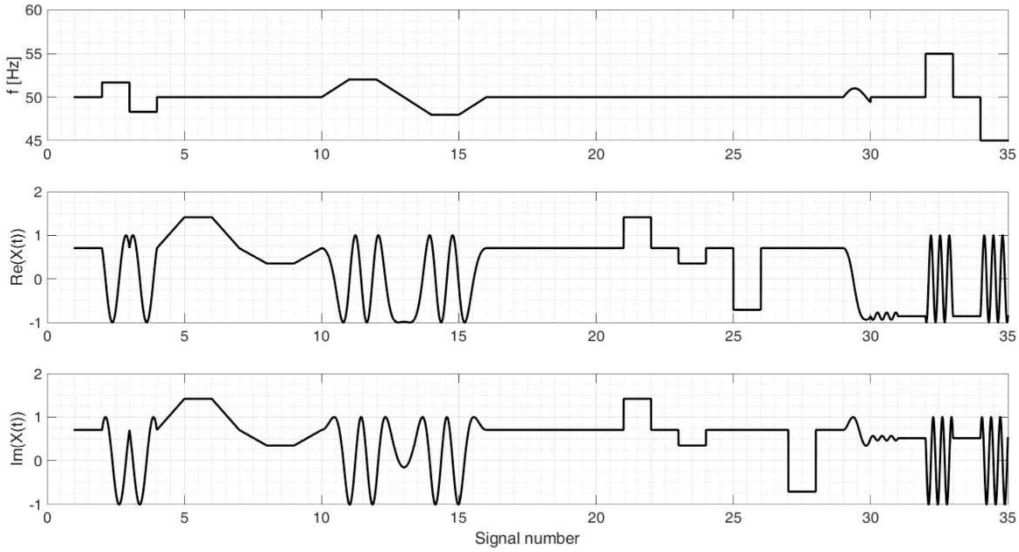

Fig. 1. Frequency, real part and imaginary part of testing phasor

4. FOURIER TRANSFORM BASED ALGORITHM

4.1. FOURIER ANALYSIS

Let us consider the set of test functions (1). According to Fourier series theory, each periodic sufficiently smooth function $x(t)$ with the angular speed ω can be represented as Fourier series formulated as follows

$$x(t) = \sum_{k=-\infty}^{\infty} a_k e^{i\omega kt} \tag{16}$$

Fourier coefficients are obtained from

$$a_k = \int_D x(t) e^{i\omega kt} \tag{17}$$

where D denotes a window length. Typically, D is equal to the integer number of periods.

For functions with constant, amplitude, phase and the nominal frequency of 50 Hz, normalized phasor can be expressed as first term in Fourier series a_1, or its conjugation a_{-1}. The fundamental idea for STFT is to extend phasor estimation as a_1 coefficient for each function in the model function set. Unfortunately, applying Eq. (17) to functions with varying amplitude or varying phase shift yields to high errors of phasor estimation. Functions with an amplitude and a phase time dependent are no longer periodic with frequency of 50 Hz in mathematical sense. Evaluated STFT for such signal is distorted by higher harmonics. Harmonic distortion rate is proportional to the amplitude and phase shift variability.

Fourier series algorithm can by significantly improved by modifying the window function. The application of additional filters reduces the influence of higher harmonic distortions. Formulas for the approximated phasor are as follows

$$y(t) = \int_{t-\frac{nT}{2}}^{t+\frac{nT}{2}} x(\tau) e^{i\omega\tau} g(t-\tau) \mathrm{d}\tau \tag{18}$$

where window function $g(t)$ determines the algorithm efficiency and also its static and dynamic characteristics.

In pure STFT the window function $g(t)$ is continuously equal to $1/D$, which implies the gain less or equal to one. In C37.118 [1] two base filters have been proposed for P and M class algorithms. Studying proper filter design is not a topic of this paper. For further investigations the window filter will be selected as the 2 periods triangle function of the form

$$g_T = \begin{cases} \left|1 - \frac{t}{T}\right|, & |t| \le T \\ 0, & |t| > T \end{cases} \tag{19}$$

where filter window $g_T(t)$ is designed to neutralize disturbances during linear amplitude changes. Furthermore, filter with $g_T(t)$ window function ensures perfect damping of higher harmonics distortion in input signal.

In real systems STFT is performed for finite number of probes. Integrals in expressions (17), (18), are substituted with finite sums. Fourier coefficients are calculated with following formula

$$a_k = \sum_{l=-\frac{N}{2}}^{\frac{N}{2}} x(l) e^{i\omega \frac{k}{f_p} t} \tag{20}$$

where f_p is sampling frequency. N is selected with respect to ω to keep integer values of $\frac{2\pi f_p}{\omega N}$. For algorithms with a window function the phasor is evaluated analogously from

$$y(m)=\sum_{l=m-\frac{N}{2}}^{m\frac{N}{2}} x(l)e^{i\omega\frac{k}{f_p}t} g_{\frac{N}{2}}(l-m) \quad (21)$$

The crucial issue for substituting integrals with finite sums is preserving base properties of STFT. Simply, Fourier coefficients are constant for base frequency signals of time independent amplitude and phase.

4.2. SIMULATION OUTCOMES

Results for TVE obtained on test signal are presented in Fig. 2. It can be observed that for signals of 50 Hz frequency and the constant amplitude (signals 1, 4–10, 16–28, 31 33), phasor estimation errors are almost negligible on the level of 10^{-7} p.u. Proper window design allows bypassing estimation errors for linear ramp of amplitude (signals 4–10). Crucial errors occurs for signals with frequencies other than 50 Hz (2, 3, 11, 14, 32, 34), for ramp of frequency (10, 12, 13, 15), frequency (29) and amplitude (30) fluctuations. Errors occurring due to frequency deviation have two primal components. First of all, the deviation from the base frequency increases the amount of higher harmonics in output signal as a consequence of window length mismatch. Secondly, the filter gain and the filter phase shift is not constant as is not a frequency function in the neighborhood of the base frequency. The additional compensating function which reacts against filter characteristic is required to mitigate these errors.

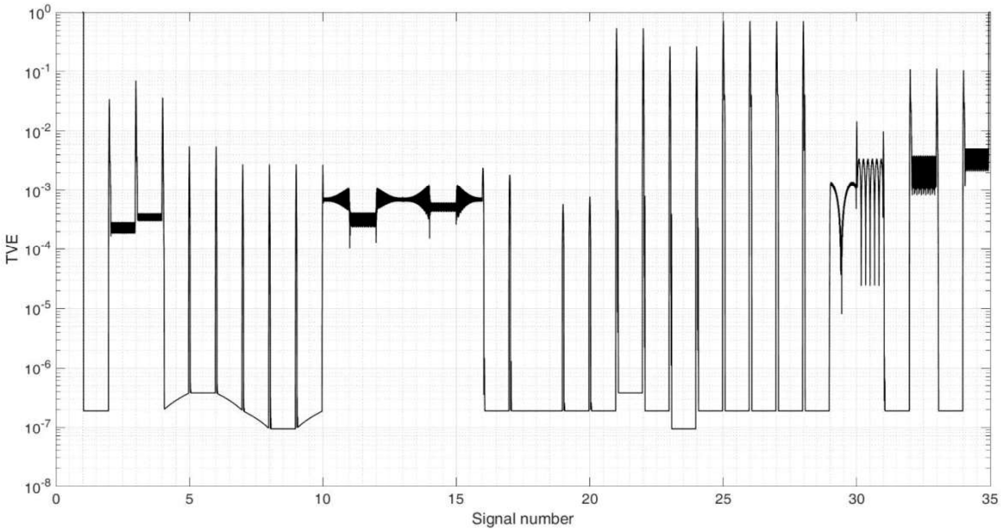

Fig. 2. Simulation results for STFT algorithm with triangle window

5. FOURIER TRANSFORM WITH PHASE LOCKED LOOP

5.1. CONTINOUS ANALYSIS

For static signals which frequencies differ from the base frequency, TVE increases rapidly when $|\Delta f|$ goes up. The primary issue for phase locked up algorithms is to reduce errors occurring due to frequency disturbance by modifying the base frequency in Fourier algorithm. STFT with the modified frequency used for phasor estimation reduces the amount of higher harmonics without disrupting orthogonality relation. The schema of the algorithm is shown in Fig. 3.

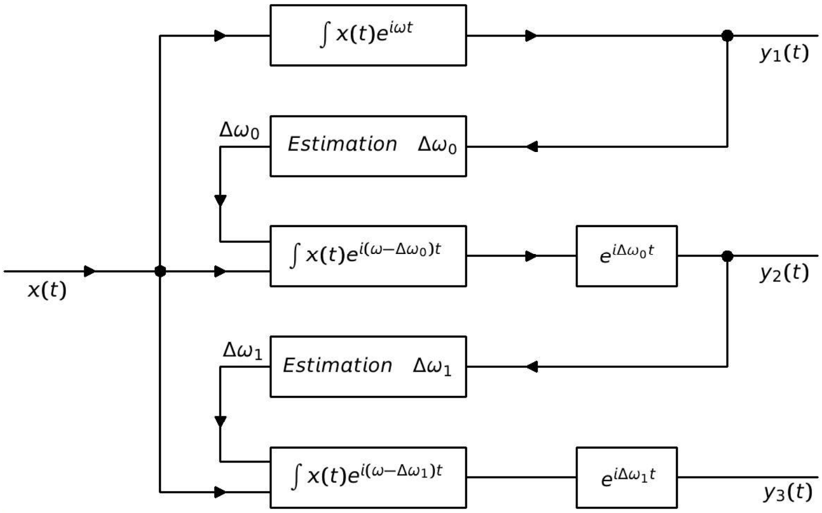

Fig. 3. Scheme of phase locked loop algorithm

For input signal $x(t)$, first phasor approximation $y_1(t)$ is evaluated using STFT.

$$y_1(t) = \int_{t-\frac{N}{2}T}^{t+\frac{N}{2}T} x(\tau)e^{i\omega\tau} g_{\frac{N}{2}T}(\tau - t)\mathrm{d}\tau \tag{22}$$

On the base of $y_1(t)$ the frequency difference between real and normalized frequency can be evaluated by using the frequency estimation algorithm. This yields to first angular speed approximation $\omega - \Delta\omega_0$. As noted above, the error rate depends on the frequency disturbance, so evaluating STFT in base angular $\omega - \Delta\omega_0$ reduces errors caused by the frequency discrepancy. Evaluating STFT in new basis requires window modification. The integration period needs to match a new angular speed. The new phasor in base $\omega - \Delta\omega_0$ is evaluated with the following formula

$$y_2(t)=\int_{t-\frac{N}{2}T_1}^{t+\frac{N}{2}T_1} x(\tau)e^{i(\omega-\Delta\omega_0)\tau}g_{\frac{N}{2}T_1}(\tau-t)\mathrm{d}\tau \tag{23}$$

where

$$T_1=\frac{1}{f-\Delta f_0}=\frac{2\pi}{\omega-\Delta\omega_0} \tag{24}$$

The phasor evaluated with STFT of modified frequency is expressed in the base of the periodic function with angular speed $\omega - \Delta\omega_0$. The normalized phasor is defined in the base of the periodic function with angular speed ω. The adjustment is obtained by rotating the second level estimation with difference frequency $\Delta\omega_0$. Phasor $y_2(t)$ obtained with this method can be used to iteratively evaluate the new frequency difference and STFT in $\omega - \Delta\omega_1$ basis. Phasor $y_3(t)$ is then calculated from

$$y_3(t)=\int_{t-\frac{N}{2}T_2}^{t+\frac{N}{2}T_2} x(\tau)e^{i(\omega-\Delta\omega_1)\tau}g_{\frac{N}{2}T_2}(\tau-t)\mathrm{d}\tau \tag{25}$$

where

$$T_1=\frac{1}{f-\Delta f_1}=\frac{2\pi}{\omega-\Delta\omega_1} \tag{26}$$

In the mathematical model, where Fourier coefficients are obtained by integrating, the sequence of iterated phasors converges to the model phasor.

5.2. DISCRETE ANALYSIS

Applications of the phase locked loop Fourier algorithm to a discrete signal suffers from the crucial problem. Discrete STFT algorithms produce errorless results as long as integration time is uniformly partitioned into probing time. To illustrate this problem let us consider the discrete input signal with the constant amplitude, the phase shift equal to 0, and with angular speed ω' which may differ from base angular speed ω. The proper phasor approximation is expected to be obtained, if angular speed ω' is known. It is necessary to know proper window length N to apply STFT with ω', however the calculated window length may not match probing frequency, what means $\frac{2\pi f_p}{\omega' N}$ isn't integer. This problem is illustrated in Fig. 4.

It follows that obtained Fourier coefficients are modified by mismatch error $f_k(E)$ which strongly depends on the reciprocal relation between ω and ω'.

$$a_k(m) = \sum_{l=m-\frac{N}{2}}^{m+\frac{N}{2}} x(l) e^{ik\omega' \frac{l}{f_p}} g_{\frac{N}{2}}(l-m) + f_k(E)(m) \tag{27}$$

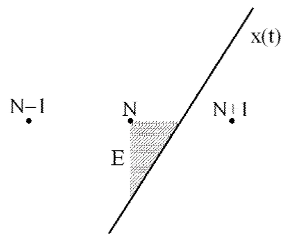

Fig. 4. Mismatch error

The mismatch error is a time varying complex valued function, which depends also on probe number m. The error can be negated by modification of window function g with respect to ω. This can be easy proven for a trivial window function used in pure STFT algorithm, however for other window functions it is much more complicated. Modifications can be performed locally, for single filter coefficient (28), or globally for multiple coefficients (29). The application of global modifications increases computational complexity but reduces vulnerability to external disturbances. It can be shown that for triangle type filter $g_{N/2}$, the mismatch error for the local compensation is expressed by

$$f_k(E)(m) = C(l) x(m-l) e^{ik\omega' \frac{m-l}{f_p}} \tag{28}$$

and for global compensation, with weighted function $D(l)$

$$f_k(E)(m) = \sum_{l=-\frac{N}{2}}^{\frac{N}{2}} C(l) x(m-l) e^{ik\omega' \frac{m-l}{f_p}} D(l) \tag{29}$$

where, $-\frac{N}{2} \le l \le \frac{N}{2}$, $C(l)$ is a complex function of l.

New filter window $g'_{N/2}$ can be obtained by modification of each l-th coefficient with weighted function $C(l)$ and the normalization process to keep the amplification less or equal to one.

Results presented in this section have been obtained for the single modification of middle filter value $C(0)$. Function $C(0)(\omega')$ is still dependent on frequency discrepancy ω'. Function $C(0)(\omega')$ graph is presented in Fig. 5. When the frequency is equal to 50 Hz, the matching condition is fulfilled and no additional compensation is necessary, i.e. compensation is equal to 0. The deviation from the base frequency increases the mismatch error, and hence the degree of compensation. Function *C* is asymmetric about 50 Hz. This is so because the area of the mismatch field is a nonlinear frequency function.

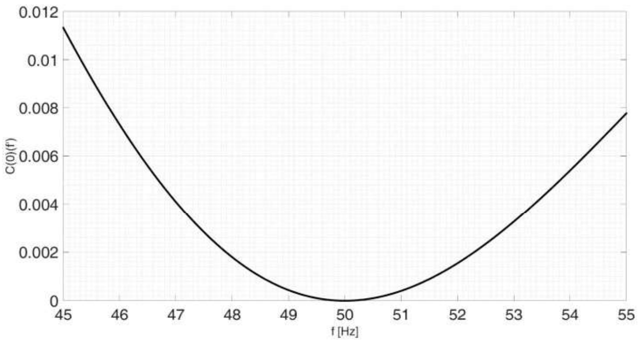

Fig. 5. Modification function for middle filter coefficient *C*(0)

5.3. SIMULATION RESULTS

Results obtained for Fourier phase locked loop algorithm are presented in Fig. 6. TVE for three levels of STFT is submitted – blue line is for pure STFT algorithm, red

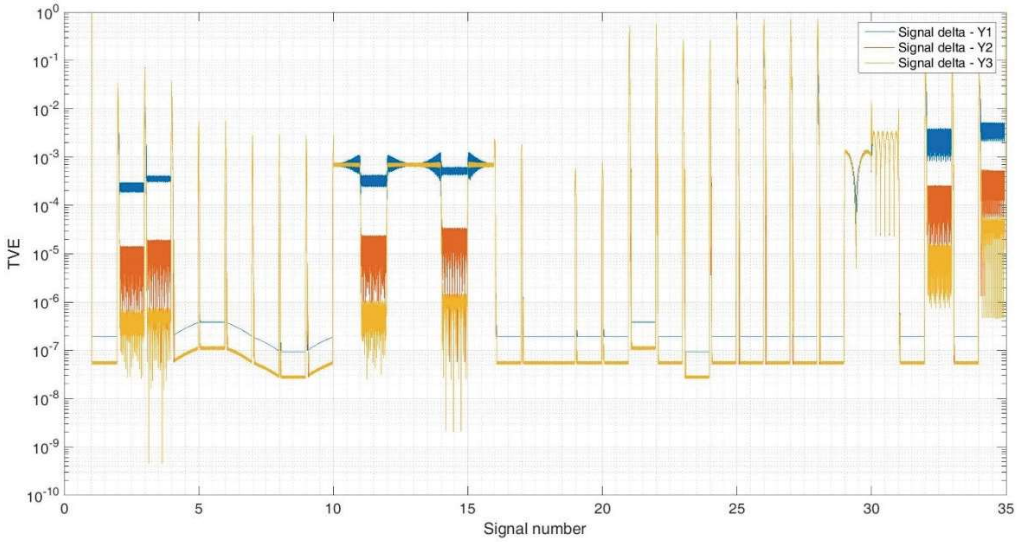

Fig. 6. Simulation results for phase locked loop STFT with triangle window

corresponds to STFT with one loop and yellow denotes a double loop. It can be observed that for signals with frequency equal to 50 Hz and constant amplitude phasors, TVE for all estimators is negligible. Minor differences between TVEs are followed by the inaccuracy in filter compensation function. Major improvement was obtained for signals with the constant frequencies differing from 50 Hz (2, 3, 11, 14, 32, 34). The first estimation (Y_1) of the phasor is burdened with heavy errors. On the basis of Y_1, the first frequency approximation was evaluated, which was closer to real vale than base 50 Hz. This approach improves the second estimation (Y_2) which is about 10 times more precise than previous one. Evaluating third approach (Y_3) allows achieving the accuracy that is comparable with the accuracy for a signal with the base frequency of 50 Hz. The further iterating lock loop process is groundless, because frequency mismatch errors are dominated by errors deriving from the magnitude and phase compensation inaccuracy. Estimation errors are preserved on the negligible level for signals with harmonic distortion (16-20), caused by retaining the orthogonality relation in multilevel STFT algorithm.

It can be observed that for signals with ramp of frequency (11, 12, 13, 15) as well as for the frequency (29) and amplitude fluctuation (30), iterative phasor evaluation does not efficiently improve the algorithm accuracy. For ramp of frequency, TVE is kept on the level corresponding to ramps around 50 Hz for the full frequency spectrum. For signals with parameter fluctuations all three phasors show the same error level. This is because estimated signals are fluctuating near the frequency of 50 Hz.

6. TAYLOR FOURIER SERIES ALGORITHM

6.1. TAYLOR SERIES EXPANSION

Taylor series expansion has been introduced to improve phasor estimation for amplitude and phasor estimation. Let us consider a function $x(t)$ with corresponding phasor $X(t)$. By phasor definition the following equation holds

$$x(t) = \mathrm{Re}(X(t)e^{i\omega t}) = \frac{X(t)e^{i\omega t} + \overline{X(t)e^{i\omega t}}}{2} \tag{30}$$

where $\overline{X(t)}$ denotes conjugation. According to Weierstrass approximation theorem, phasor $X(T)$ can be approximated with N – order complex polynomial as follows

$$X(T) \approx \sum_{k=0}^{N} a_k t^k = \mathbf{AT} = \sum_{k=0}^{N} b_k p_k(t) = \mathbf{BP}(t)$$

$$\mathbf{A} = (a_0 \quad a_1 \quad \ldots \quad a_{N-1} \quad a_N)$$

$$\mathbf{B} = (b_0 \quad b_1 \quad \ldots \quad b_{N-1} \quad b_N) \tag{31}$$

$$\mathbf{T} = (1 \quad t \quad \ldots \quad t^{N-1} \quad t^N)$$

$$\mathbf{P}(t) = (p_0(t) \quad p_1(t) \quad \ldots \quad p_{N-1}(t) \quad p_N(t))$$

where coefficients a_k are complex numbers. By choosing the set of polynomials $p_k(t)$, (31) can be expressed as a sum of polynomials, where $p_k(t)$ is a polynomial of order k. The problem can be formulated as

$$x(t) \approx \frac{\mathbf{BP}e^{i\omega t} + \overline{\mathbf{B}}\mathbf{P}e^{-i\omega t}}{2} = \frac{1}{2}(\mathbf{B} \quad \overline{\mathbf{B}})\begin{pmatrix} \mathbf{P}(t)e^{i\omega t} \\ \mathbf{P}(t)e^{-i\omega t} \end{pmatrix} \tag{32}$$

Multiplying both sides of (32) by transposition of $\begin{pmatrix} \mathbf{P}(t)e^{i\omega t} \\ \mathbf{P}(t)e^{-i\omega t} \end{pmatrix}$ we obtain

$$x(t)(\mathbf{P}'(t)e^{i\omega t} \quad \mathbf{P}'e^{-i\omega t}) \approx \frac{1}{2}(\mathbf{B} \quad \overline{\mathbf{B}})\begin{pmatrix} \mathbf{P}(t)\mathbf{P}'(t)e^{i2\omega t} & \mathbf{P}(t)\mathbf{P}'(t) \\ \mathbf{P}(t)\mathbf{P}'(t) & \mathbf{P}(t)\mathbf{P}'(t)e^{-i2\omega t} \end{pmatrix} \tag{33}$$

In order to obtain the polynomial approximation of the phasor, matrix (**B** conj(**B**)) has to be evaluated. The matrix on the right hand side consists complex functions, which columns are linearly dependent. It follows that the matrix is irreversible for any t. To obtain the linear dependence it is sufficient to transform the matrix of functions into the matrix of numbers, and to ensure the linear independence. The integration of both sides of (33) Yields

$$\int x(t)(\mathbf{P}'(t)e^{i\omega t} \quad \mathbf{P}'(t)e^{-i\omega t}) \approx \frac{1}{2}(\mathbf{B} \quad \overline{\mathbf{B}})\int\begin{pmatrix} \mathbf{P}(t)\mathbf{P}'(t)e^{i2\omega t} & \mathbf{P}(t)\mathbf{P}'(t) \\ \mathbf{P}(t)\mathbf{P}'(t) & \mathbf{P}(t)\mathbf{P}'(t)e^{-i2\omega t} \end{pmatrix} \tag{34}$$

The proper set of polynomials P simplifies the expression, giving

$$\int x(t)(\mathbf{P}'(t)e^{i\omega t} \quad \mathbf{P}'e^{-i\omega t}) \approx \frac{1}{2}(\mathbf{B} \quad \overline{\mathbf{B}})\begin{pmatrix} \int \mathbf{P}(t)\mathbf{P}'(t)e^{i2\omega t} & I \\ I & \int \mathbf{P}(t)\mathbf{P}'(t)e^{-i2\omega t} \end{pmatrix} \tag{35}$$

The multiplication of (35) by the inverse matrix gives

$$\frac{1}{2}(\mathbf{B} \quad \overline{\mathbf{B}}) \approx \int x(t)(\mathbf{P}'(t)e^{i\omega t} \quad \mathbf{P}'e^{-i\omega t})\begin{pmatrix} \int \mathbf{P}(t)\mathbf{P}'(t)e^{i2\omega t} & I \\ I & \int \mathbf{P}(t)\mathbf{P}'(t)e^{-i2\omega t} \end{pmatrix} \quad (36)$$

The dynamic phasor estimated integrating time domain is expressed as (31). The immediate phasor value for time $t = 0$ is obtained as b_0, i.e. first element in matrix **B**.

6.2. SIMULATION RESULTS

Results obtained for Fourier Taylor series algorithm are depicted in Fig. 7. Analysis has been performed for polynomials of order 2 (blue), 4 (red) and 6 (yellow). It can be observed that for signals with the base frequency of 50 Hz and without higher harmonic distortion (1, 4–9, 20–28, 31, 33), the best estimation accuracy is achieved for any polynomial order, the same as for STFT algorithms. For signals with frequency disturbances, liner frequency changes, as well as frequency and amplitude fluctuations (2, 3, 10-15, 29, 30, 32, 34), increasing polynomial order improves the estimation efficiency. For the signal with the higher harmonics content (16–19) the occurring error is higher. It follows form both the property of LSM and the non-uniqueness of the phasor. Each signal with higher harmonic distortion can be formulated as a dynamic phasor without higher harmonics but with varying amplitude and/or varying phase shift. This phasor is approximated by a polynomial instead of being damped.

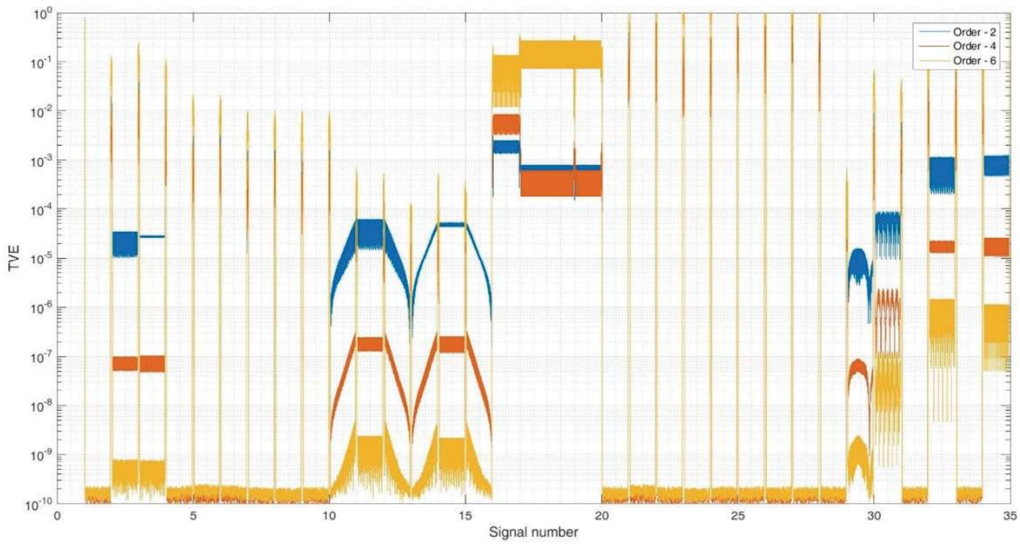

Fig. 7. Simulation results for Taylor-Fourier series method

Therefore, for the pure Taylor series algorithm the orthogonality relation no longer holds. Orthogonality can be ensured by extending the function base with complex functions with higher frequency $P(t)e^{ik\omega t}$, for $k > 1$. The best suiting polynomial form of the approximation is determined by the required algorithm accuracy, the acceptable computational complexity, and the capability of inverse matrix evaluation.

7. CONCLUSION

This work has shown reasons of synchrophasor estimation errors in electrical power systems. STFT and Fourier Taylor series based algorithms were studied to determine their advantages and disadvantages as well as possibilities for further efficiency improvement.

Investigations have revealed that algorithms based on STFT as well as phase locked algorithms are efficient as long as amplitude and frequency of the processed signal are constant. According to previous phasor analysis one signal can have many phasor representations. It follows that the signal with varying amplitude and/or frequency, can be considered as different signals with the harmonic distortion. In consequence, important signal parameters are being expressed as higher harmonics. As higher harmonics are damped by applied filters, some signal information is lost in the phasor representation.

Efficiency of Taylor Fourier series based algorithms strongly depends on the polynomial order adopted for the phasor approximation. Firstly, appropriate selection of the polynomial order is strongly determined by accuracy requirements, restrictions on the response overshoot and the capability of the harmonic distortion damping. Secondly, properties of the integration process in Taylor Fourier method need to be well stated. By modifying the integrating function in LSM, dedicated properties can be acquired. The estimation accuracy can be improved also by substituting polynomial approximation by the nonlinear approximation and by modification of LSM, however further research needs to be conducted.

REFERENCES

[1] IEEE Standard for Synchrophasor Measurements for Power Systems, IEEE Standard C37.118.1-2011, Dec. 2011.

[2] MACII D., BARCHI G., PETRI D., *Design Criteria of Digital Filters for Synchrophasor Estimation*, Instrumentation and Measurement Technology Conference (I2MTC), 2013 IEEE International, Minneapolis, MN, USA, 2013.

[3] ROMANO P., PAOLONE M., *Enhanced Interpolated-DFT for Synchrophasor Estimation in FPGAs: Theory, Implementation, and Validation of a PMU Prototype*, IEEE Transactions on Instrumentation and Measurement, December 2014, Vol. 63, No. 12.

[4] ROSCOE A.J., ABDULHADI I.F., BURT G.M., *P-Class Phasor Measurement Unit Algorithms Using Adaptive Filtering to Enhance Accuracy at OffNominal Frequencies*, IEEE International Conference on Smart Measurements for Future Grids (SMFG), Bologna, Italy, 2011.

[5] ROSCOE A.J., ABDULHADI I.F., BURT G.M., *P and M Class Phasor Measurement Unit Algorithms Using Adaptive Cascaded Filters*, IEEE Transactions on Power Delivery, July 2013, Vol. 28, No. 3.
[6] PLATAS-GARZ M., SERNA J., *Dynamic Phasor and Frequency Estimates through Maximally Flat Differentiators*, IEEE Transactions on Instrumentation and Measurement, July 2010, Vol. 59, No. 7.
[7] MAI R.K., HE Z.Y., FU L., KIRBY B., BO Z.Q., *A Dynamic Synchrophasor Estimation Algorithm for Online Application*, IEEE Transactions on Power Delivery, April 2010, Vol. 25, No. 2.
[8] BELEGA D., FONTANELLI D., PETRI D., *Low-Complexity Least-Squares Dynamic Synchrophasor Estimation Based on the Discrete Fourier Transform*, IEEE Transactions on Instrumentation and Measurement, December 2015, Vol. 64, No. 12.
[9] SERNA J., *Synchrophasor Measurement with Polynomial Phase-Locked-Loop Taylor–Fourier Filters*, IEEE Transactions on Instrumentation and Measurement, February 2015, Vol. 64, No. 2.
[10] FU L., ZHANG J., XIONG S., HE Z., MAI R., *A Modified Dynamic Synchrophasor Estimation Algorithm Considering Frequency Deviation*, IEEE Transactions on Smart Grid, March 2017, Vol. 8, No. 2.